

# Separation of CO<sub>2</sub> and H<sub>2</sub>S using room-temperature ionic liquid [bmim][PF<sub>6</sub>]

Mark B. Shiflett<sup>a,\*</sup>, A. Yokozeki<sup>b</sup>

<sup>a</sup> DuPont Central Research and Development, Experimental Station, Building E304/A320 Route 141, Wilmington, DE 19880, USA

<sup>b</sup> 109-C Congressional Drive, Wilmington, DE 19807, USA

## ARTICLE INFO

### Article history:

Received 1 November 2009

Received in revised form 16 January 2010

Accepted 18 January 2010

Available online 25 January 2010

### Keywords:

Carbon dioxide

Hydrogen sulfide

Gas solubility

Ionic liquid

Equation of state

Phase equilibria

Liquid–liquid separation

Gas separation

## ABSTRACT

We have developed a ternary equation of state (EOS) model for the CO<sub>2</sub>/H<sub>2</sub>S/1-butyl-3-methylimidazolium hexafluorophosphate ([bmim][PF<sub>6</sub>]) system in order to understand the separation of these gases using room-temperature ionic liquids (RTILs). The present model is based on a generic RK (Redlich-Kwong) EOS, with empirical interaction parameters for each binary system. These interaction parameters have been determined using our previously measured VLE (vapor–liquid equilibrium) data for CO<sub>2</sub>/[bmim][PF<sub>6</sub>] and literature data for H<sub>2</sub>S/[bmim][PF<sub>6</sub>] and CO<sub>2</sub>/H<sub>2</sub>S. VLLE (vapor–liquid–liquid equilibrium) measurements have been made and validate EOS model predictions which suggest that the CO<sub>2</sub>/[bmim][PF<sub>6</sub>] and H<sub>2</sub>S/[bmim][PF<sub>6</sub>] systems are Type V phase behavior, according to the classification of van Konynenburg and Scott. The validity of the ternary EOS model calculations has also been checked by conducting VLE experiments for the CO<sub>2</sub>/H<sub>2</sub>S/[bmim][PF<sub>6</sub>] system. With this EOS model, isothermal ternary phase diagrams and solubility (VLE) behavior have been calculated for various (*T*, *P*, and feed compositions) conditions. The CO<sub>2</sub>/H<sub>2</sub>S gas selectivity is nearly independent of the amount of ionic liquid addition and ranged from about 3.2 to 4.0. For large CO<sub>2</sub>/H<sub>2</sub>S mole ratios (9/1) at 298.15 K, the addition of the ionic liquid increases the CO<sub>2</sub>/H<sub>2</sub>S gas selectivity from about 1.2 to 3.7. For high temperature (333.15 K) and high CO<sub>2</sub>/H<sub>2</sub>S feed ratios, the addition of the ionic liquid provides the only means of separation because no VLE exists for the CO<sub>2</sub>/H<sub>2</sub>S binary system without the ionic liquid.

© 2010 Elsevier B.V. All rights reserved.

## 1. Introduction

Hydrogen sulfide (H<sub>2</sub>S) and carbon dioxide (CO<sub>2</sub>) are commonly removed from natural and synthesis gases through chemical absorption using aqueous solutions of organic bases like single amines, amine mixtures, or mixtures of an amine and a salt of an amino acid [1,2]. Extensive research has been conducted by several groups on aqueous solutions of alkanolamines, especially monoethanolamine (MEA), diethanolamine (DEA) and methyldiethanolamine (MDEA) for natural gas treating and sweetening [3–13]. The typical process involves competitive chemical absorption of H<sub>2</sub>S and CO<sub>2</sub> in a packed column at low temperature (preferably ambient temperature) and elevated pressures (up to about 4 MPa or more). The gas desorption or solvent regeneration occurs at elevated temperatures (typically around 350–400 K) and low pressures using a stripping column. Disadvantages of aqueous solutions of alkanolamines include loss of the amine during regeneration, transfer of water into the gas stream, degradation of the amine to form corrosive byproducts, and low temperature and high pressure absorption, all of which makes this process economically expensive.

Room-temperature ionic liquids (RTILs) have been proposed for the capture of gases such as CO<sub>2</sub>. Several solubility studies of CO<sub>2</sub> in many RTILs have been reported [14–27]; however only a few researchers have examined the binary phase *PT<sub>x</sub>* (pressure–temperature composition) behavior of H<sub>2</sub>S in ionic liquids [28–31]. Jou and Mather [28] reported the first solubility data of H<sub>2</sub>S in 1-butyl-3-methylimidazolium hexafluorophosphate ([bmim][PF<sub>6</sub>]) at temperatures from 298.15 to 403.15 K and pressures up to 9.6 MPa. Pomelli et al. [29] measured the solubility of H<sub>2</sub>S in different imidazolium-based ionic liquids with various anions and in a series of bis(trifluoromethyl)sulfonylimide (Tf<sub>2</sub>N)-based ionic liquids with various cations at 298.15 K and 1400 kPa. Heintz et al. [30] attempt to measure the solubility of CO<sub>2</sub> and a mixture of N<sub>2</sub>/H<sub>2</sub>S in an ionic liquid with an ammonium cation and chloride anion from 300 to 500 K and pressures up to 2.3 and 30 bar for H<sub>2</sub>S and CO<sub>2</sub>, respectively; however the structure of the ionic liquid was unknown and an approximate chemical formula was assumed for calculating the mole fraction solubilities.

Recently, Jalili et al. [31] measured the solubility of H<sub>2</sub>S in three RTIL ([bmim][PF<sub>6</sub>], [bmim][BF<sub>4</sub>] and [bmim][Tf<sub>2</sub>N]) at temperatures from 303.15 to 343.15 K and pressures up to 1 MPa. In each case the H<sub>2</sub>S solubility is much higher compared with CO<sub>2</sub>. For example, Henry's law constants are 51.7 and 1.43 bar at 298 K for CO<sub>2</sub> and H<sub>2</sub>S in RTIL ([bmim][PF<sub>6</sub>]), respectively [17,31]. This large difference in the Henry's law constant suggests the selective cap-

\* Corresponding author. Tel.: +1 302 695 2572; fax: +1 302 695 4414.  
E-mail address: [mark.b.shiflett@usa.dupont.com](mailto:mark.b.shiflett@usa.dupont.com) (M.B. Shiflett).

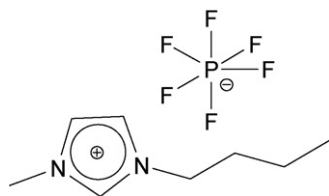


Fig. 1. Chemical structure of [bmim][PF<sub>6</sub>].

turing and separation of these gases may be possible using ionic liquids.

In the present study, we construct for the first time the ternary phase diagrams of CO<sub>2</sub>/H<sub>2</sub>S/[bmim][PF<sub>6</sub>], using our cubic equation-of-state (EOS) method [14,32]. The ternary EOS is based on interaction parameters of each binary system, and the binary interaction parameters were determined from our previous VLE (vapor–liquid equilibrium) measurements for CO<sub>2</sub>/[bmim][PF<sub>6</sub>] [17], and literature data for H<sub>2</sub>S/[bmim][PF<sub>6</sub>] [28] and CO<sub>2</sub>/H<sub>2</sub>S [13]. We have also measured the VLE for the CO<sub>2</sub>/[bmim][PF<sub>6</sub>] and H<sub>2</sub>S/[bmim][PF<sub>6</sub>] binary systems to validate the boundary of the immiscibility region.

In order to check the validity of the ternary EOS, VLE experiments for the CO<sub>2</sub>/H<sub>2</sub>S/[bmim][PF<sub>6</sub>] system were performed under various *T*, *P*, and feed compositions, and the EOS validity was satisfactorily confirmed. Then, the CO<sub>2</sub>/H<sub>2</sub>S selectivity with and without RTIL [bmim][PF<sub>6</sub>] are calculated at several feed, *T*, and *P* conditions. The selectivity advantage using this RTIL is discussed based on the present ternary phase calculations.

## 2. Experimental

### 2.1. Materials

Hydrogen sulfide (mole fraction purity >0.995, CAS no. 7783-06-4) and carbon dioxide (mole fraction purity >0.9999, CAS no. 124-38-9) were purchased from MG Industries (Philadelphia, PA). The [bmim][PF<sub>6</sub>] (C<sub>8</sub>H<sub>15</sub>N<sub>2</sub>F<sub>6</sub>P, Lot and filling number 1242554 15005226, CAS no. 174501-64-5) was obtained from Fluka (Buchs, Switzerland). Fig. 1 provides the chemical structure. The [bmim][PF<sub>6</sub>] ionic liquid sample was dried and degassed by first placing the sample in a borosilicate glass tube and pulling a vacuum on the sample with a diaphragm pump (Pfeiffer, model MVP055-3) for about 3 h. Next, the sample was fully evacuated using a turbopump (Pfeiffer, model TSH-071) to a pressure of about  $4 \times 10^{-7}$  kPa while simultaneously heating and stirring the ionic liquid at a temperature of about 348 K for 5 days. The final water content was measured by Karl-Fischer titration (Aqua-Star C3000, solutions AquaStar Coulomat C and A) and the ionic liquid contained 482 ppm of water (mass basis).

### 2.2. Binary VLE measurements

In our previous report, we measured the gas solubility of CO<sub>2</sub> and [bmim][PF<sub>6</sub>] using a gravimetric microbalance [17] (Hidden Isochema Ltd., IGA 003). Detailed descriptions of the experimental equipment and procedures for the VLE are given in our previous reports [17,33]. Solubility data for H<sub>2</sub>S and [bmim][PF<sub>6</sub>] were taken from Jou and Mather [28]; however not all the data were used. We excluded from our analysis the last two data points at 298.15 K and the last data point at other temperatures (e.g. 313.15 and 343.15 K) shown in Ref. [28] because these were determined using the NIST REFPROP EOS program [34] to be in the VLLE region. The CO<sub>2</sub>/H<sub>2</sub>S data were taken from Bierlein and Kay [13].

### 2.3. Binary VLLE measurements

Seven high-pressure sample containers were filled with dried [bmim][PF<sub>6</sub>] following the procedures outlined in our previous publications [35,36]. Two samples were filled with liquid CO<sub>2</sub> and contained about 74.2 and 95.5 mol% CO<sub>2</sub>. Five samples were filled with liquid H<sub>2</sub>S and contained about 89.2, 93.2, 95.4, 98.4 and 99.2 mol% H<sub>2</sub>S. Hydrogen sulfide is classified as an extremely hazardous gas and caution must be used when handling. Hydrogen sulfide is flammable and highly toxic with an 8–12 h allowable exposure limit (AEL) of 10 ppm. In our experiment, the H<sub>2</sub>S cylinder and samples were always handled and stored in a ventilated hood. Proper personal protective equipment was worn when preparing and handling samples and all materials were disposed of by incineration. Hydrogen sulfide has a strong odor which is easily detectable (0.0047 ppm odor threshold); however, loss of sensitivity is known to occur after initial exposure; therefore, all employees were also required to wear air-monitoring badges (Morphix, part no. 382015-50, Virginia Beach, VA) which could detect H<sub>2</sub>S at 0.25 ppm when working in the laboratory.

VLLE experiments have been made with these samples at constant temperatures from about 283 to 293 K for CO<sub>2</sub> + [bmim][PF<sub>6</sub>] and 273 to 342 K for H<sub>2</sub>S + [bmim][PF<sub>6</sub>] using the volumetric method [35,36]. The VLLE determined by this method required only mass and volume measurements without any analytical method for molar composition or chemical analysis. Special attention must be given to ensure no leaks occur from the sample containers after being filled with the high-pressure CO<sub>2</sub> and H<sub>2</sub>S. Weights of sample containers were checked several times before starting and after completing the VLLE experiments to quantify whether any CO<sub>2</sub> or H<sub>2</sub>S had escaped from the sample container. The samples were placed inside a constant temperature water bath and were mechanically mixed while immersed in the tank [35]. The bath temperature was calibrated using a standard platinum resistance thermometer (SPRT model 5699, Hart Scientific, range 73–933 K) and readout (Blackstack model 1560 with SPRT module 2560). The Blackstack instrument and SPRT are a certified secondary temperature standard with a NIST traceable accuracy to  $\pm 0.005$  K. The uncertainty in the bath temperature was 0.2 K.

One of the most useful aspects of the present VLLE method is the ability to obtain the molar volume of each separated liquid simultaneously with the mole fraction of each liquid at any given isothermal condition. Then, the excess molar volume (or volume of mixing) of each liquid solution ( $V^E$  and  $V^E$ ) can be obtained, by use of the pure component molar volumes  $V_1^0$  (CO<sub>2</sub> or H<sub>2</sub>S) and  $V_2^0$  ([bmim][PF<sub>6</sub>]) using:

$$V^E = V_m - x'_1 V_1^0 - x'_2 V_2^0 \quad \text{or} \quad V^E = V_m - x_1 V_1^0 - x_2 V_2^0, \quad (1)$$

where  $V_m$  is the measured molar volume of the mixture ( $V'_m$  for the lower phase *L'* or  $V_m$  for the upper phase *L*), and ( $x'_1, x'_2$  or  $x_1, x_2$ ) are mole fractions of CO<sub>2</sub> or H<sub>2</sub>S (1) and [bmim][PF<sub>6</sub>] (2) in phases *L'* and *L*, respectively. Saturated liquid molar volumes for CO<sub>2</sub> and H<sub>2</sub>S were calculated using the NIST REFPROP EOS program [34]. The molar volume for [bmim][PF<sub>6</sub>] was calculated from known liquid density data [17].

It is important to mention that the vapor phase density which contains CO<sub>2</sub> or H<sub>2</sub>S with a negligible contribution of [bmim][PF<sub>6</sub>] must be properly accounted for in the mass balance equations. Observed liquid phase compositions and molar volumes for CO<sub>2</sub> + [bmim][PF<sub>6</sub>] and H<sub>2</sub>S + [bmim][PF<sub>6</sub>] are shown in Tables 1 and 2, respectively. Total uncertainties ( $\delta x_{TE} = \sqrt{\delta x_{RE}^2 + \delta x_{SE}^2}$ ) were estimated by calculating both the overall random ( $\delta x_{RE}$ ) and systematic errors ( $\delta x_{SE}$ ). The following experimental parameters were considered to have an effect on the random errors: sample container calibration constants, mass of

**Table 1**  
Experimental VLE for CO<sub>2</sub> (1) + [bmim][PF<sub>6</sub>] (2).

T/K	$x_1'$ /mol%	$x_1$ /mol%	$\bar{V}^a/\text{cm}^3 \text{ mol}^{-1}$	$\bar{V}^b/\text{cm}^3 \text{ mol}^{-1}$	$\bar{V}^{\text{ex}b}/\text{cm}^3 \text{ mol}^{-1}$	$\bar{V}^{\text{ex}b}/\text{cm}^3 \text{ mol}^{-1}$
283.1	61.1 ± 1.0	100.0–0.4	105.1 ± 1.5	51.0 ± 1.0	–6.2 ± 1.5	–0.1 ± 1.0
293.0	59.7 ± 1.0	100.0–0.4	106.2 ± 1.5	57.3 ± 1.0	–9.7 ± 1.5	–0.2 ± 1.0

<sup>a</sup> Observed molar volume.

<sup>b</sup> Excess molar volume.

**Table 2**  
Experimental VLE for H<sub>2</sub>S (1) + [bmim][PF<sub>6</sub>] (2).

T/K	$x_1'$ /mol%	$x_1$ /mol%	$\bar{V}^a/\text{cm}^3 \text{ mol}^{-1}$	$\bar{V}^b/\text{cm}^3 \text{ mol}^{-1}$	$\bar{V}^{\text{ex}b}/\text{cm}^3 \text{ mol}^{-1}$	$\bar{V}^{\text{ex}b}/\text{cm}^3 \text{ mol}^{-1}$
273.6	92.3 ± 2.5	98.9 ± 0.5	51.5 ± 2.0	41.0 ± 1.4	–2.1 ± 2.0	–1.8 ± 1.4
282.8	89.8 ± 2.4	99.2 ± 0.5	54.0 ± 2.5	42.0 ± 1.3	–4.7 ± 2.5	–1.3 ± 1.3
294.6	88.5 ± 2.3	99.5 ± 0.5	56.9 ± 2.4	43.5 ± 1.2	–5.5 ± 2.4	–0.9 ± 1.2
309.6	85.8 ± 2.2	99.6 ± 0.4	61.4 ± 2.0	45.7 ± 1.1	–7.5 ± 2.0	–0.7 ± 1.1
325.2	84.0 ± 2.1	99.7 ± 0.3	66.0 ± 1.8	48.8 ± 1.0	–8.7 ± 1.8	–0.4 ± 1.0
342.2	82.1 ± 2.1	100.0–0.4	71.0 ± 1.8	53.3 ± 1.0	–10.9 ± 1.8	0.0 ± 1.0

<sup>a</sup> Observed molar volume.

<sup>b</sup> Excess molar volume.

CO<sub>2</sub>, H<sub>2</sub>S and [bmim][PF<sub>6</sub>], height of lower and upper phases. The heights had the largest overall effect. The systematic errors include properly correcting for the sample level, area expansion, meniscus, and vapor phase moles. For additional details on estimation of total errors see Refs. [35,36].

In order to understand the boundary of the VLE curve for CO<sub>2</sub>/[bmim][PF<sub>6</sub>] and H<sub>2</sub>S/[bmim][PF<sub>6</sub>], an attempt was made to measure the cloud-points with the binary mixtures containing mole fractions of 74.2 and 95.5% CO<sub>2</sub> + [bmim][PF<sub>6</sub>] and 93.2, and 95.4% H<sub>2</sub>S + [bmim][PF<sub>6</sub>]. Starting at ambient temperature of about 293 K, two liquid phases existed and the temperature was lowered with manual mixing in a constant temperature bath of methanol and dry ice to about 198 K. One of these samples (93.2 mol% H<sub>2</sub>S + [bmim][PF<sub>6</sub>]) became single phase at 198 K. The temperature of the single-phase sample was slowly raised (1 K/min) until a cloud layer became visible inside the high-pressure sample container. The temperature was recorded when the cloud layer formed. The liquid level in the tube at the cloud point temperature must also be measured in order to calculate the vapor phase volume. The vapor is assumed to contain only H<sub>2</sub>S and using an EOS program [34] the saturated vapor density was calculated at the cloud point temperature to correct the amount of H<sub>2</sub>S in the liquid phase (reported cloud point composition).

#### 2.4. Ternary VLE measurements

We have also conducted VLE experiments for the present ternary system (CO<sub>2</sub>/H<sub>2</sub>S/[bmim][PF<sub>6</sub>]) at several thermodynamic conditions in order to verify the present EOS model.

Five sample cells have been constructed as shown in Fig. 2. Each cell was made using Swagelok fittings, two Swagelok valves (valve 1 is a stem valve, part number SS-4JB1 and valve 2 is a ball valve, part number SS-426S4), a stainless steel cylinder, and a pressure gauge (Parker Instruments, 0–0.75 MPa). The internal volume of each cell was calculated by measuring the mass of methanol required to completely fill the cell and knowing the density of methanol at the fill temperature. The internal volume of each cell ( $V_T$ ) was 90 ± 2.5 cm<sup>3</sup>. Ionic liquid was loaded by mass (0.61–7.14 g) and weighed on an analytical balance with a resolution of 0.01 g (Mettler Toledo PG-4002-S) inside a nitrogen purged dry box. In order to load ionic liquid in the cell, the pressure gauge, valves and fittings were removed and a glass pipette (10 ml) which fit through the cylinder opening was used for filling. The pressure gauge, valves and fittings were assembled as shown in Fig. 2 and the sample cell was removed from the dry box. After filling with the ionic liq-

uid, the sample cell was always maintained in a vertical upright position when valve 1 was open to prevent ionic liquid coming in contact with the valves and pressure gauge. If the sample cell had to be mixed or weighed in a horizontal position, valve 1 would be closed and then once in the vertical position opened again. The cell was connected to the diaphragm pump, with both valves open, to remove residual nitrogen. After the cell was evacuated, the ball valve (valve 2) was closed and the cell was weighed to obtain the initial ionic liquid mass.

The CO<sub>2</sub>/H<sub>2</sub>S gas mixtures were also loaded by mass (0.57–0.72 g) from a high-pressure gas cylinder. Three CO<sub>2</sub>/H<sub>2</sub>S gas mixtures (9.5/90.5, 54.6/45.4, and 90.4/9.6 mol% CO<sub>2</sub>/H<sub>2</sub>S) were prepared by weight and analyzed by gas chromatography (GC) (Hewlett Packard HP6890) using an isothermal (80 °C) method (GS-GASPRO capillary column, 60 m length, 0.32 mm I.D., model 113-4362, Agilent Technologies, inlet injector temperature 200 °C, thermal conductivity detector temperature 250 °C, helium carrier

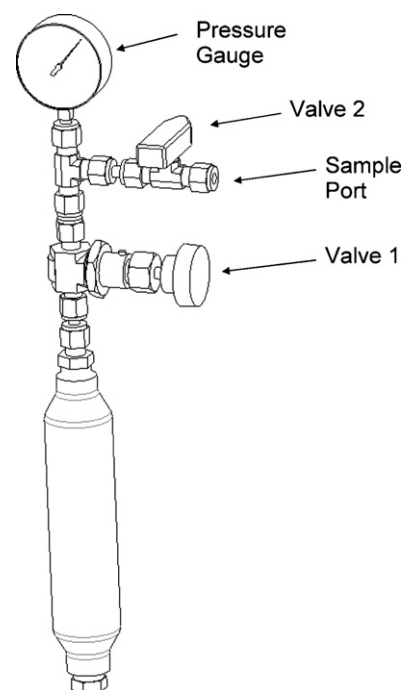


**Fig. 2.** Schematic diagram of a sample cell.

gas, flow rate  $55 \text{ cm}^3 \text{ min}^{-1}$  with a 20:1 split ratio, injection volume  $25 \mu\text{L}$ . Special care must be taken when preparing the  $\text{CO}_2/\text{H}_2\text{S}$  gas mixtures to prevent the  $\text{H}_2\text{S}$  from condensing. The saturation vapor pressure for  $\text{CO}_2$  at 293 K is 6.0 MPa; however, the saturation pressure for  $\text{H}_2\text{S}$  at 293 K is lower at 1.78 MPa. Therefore, the total pressure for the three gas mixtures (9.5/90.5, 54.6/45.4, 90.4/9.6 mol%  $\text{CO}_2/\text{H}_2\text{S}$ ) were 1.07, 1.07, and 1.03 MPa, respectively.

The sample cells were placed inside a Plexiglas tank and the temperature was controlled with an external temperature bath (VWR International, Model 1160S) which circulated water through a copper coil inside the tank. The bath was stirred with an agitator (Arrow Engineering Co., Inc. model 1750) and the temperature measured with a thermocouple (Fluke 52II thermometer). The temperature was initially set at about 296 K. The sample cells were vigorously shaken to assist with mixing prior to being immersed in the tank. The water level in the tank was adjusted such that the entire cell was under water including the bottom 2 cm of the pressure gauge. The pressure in each cell was recorded until no change in pressure was measured. To ensure the samples were at equilibrium and properly mixed, the cells were momentarily removed from the water bath and vigorously shaken. The cells were placed back in the bath and the process was repeated until no change in pressure was measured. In most cases the cells reached equilibrium in 12 to 24 h. The process was repeated at a higher temperature of about 322 K.

The pressure gauges were calibrated using the Paroscientific Model 765-1K pressure transducer. The Fluke thermometer was calibrated using the standard platinum resistance thermometer (SPRT model 5699, Hart Scientific, range 73–933 K) and readout (Blackstack model 1560 with SPRT module 2560). The temperature and pressure uncertainties were  $\pm 0.2 \text{ K}$  and  $\pm 0.005 \text{ MPa}$ .

The vapor space of each sample was analyzed by placing a rubber septum over the end of the valve and inserting a gas-tight syringe (Hamilton Company, Reno, NV) to remove a small sample ( $25 \mu\text{L}$ ) which was analyzed by GC. The  $\text{CO}_2$  and  $\text{H}_2\text{S}$  peaks appeared at about 3.5 and 5.0 min, respectively with a total method run time of 7.0 min.

### 3. Thermodynamic model

In order to study the phase behavior of a ternary system of  $\text{CO}_2/\text{H}_2\text{S}/[\text{bmim}][\text{PF}_6]$ , we have developed for the first time thermodynamic models based on equations of state (EOS), which have been successfully applied for refrigerant/lubricant oil mixtures [32] and various hydrofluorocarbons and  $\text{CO}_2$  mixtures with ionic liquids [14–17,37]. It is based on a generic Redlich-Kwong (RK) type of cubic EOS:

$$P = \frac{RT}{V-b} - \frac{a(T)}{V(V+b)}, \quad (2)$$

$$a(T) = 0.427480 \frac{R^2 T_c^2}{P_c} \alpha(T), \quad (3)$$

$$b = 0.08664 \frac{RT_c}{P_c}. \quad (4)$$

The temperature-dependent part of the  $a$  parameter in the EOS for pure compounds is modeled by the following empirical form [14–17,37]:

$$\alpha(T) = \sum_{k=0}^{\leq 3} \beta_k \left( \frac{1}{T_r} - T_r \right)^k \quad \left( T_r \equiv \frac{T}{T_c} \right), \quad (5)$$

The coefficients,  $\beta_k$ , are determined so as to reproduce the vapor pressure of each pure compound.

The  $a$  and  $b$  parameters for general  $N$ -component mixtures are modeled in terms of their respective binary interaction parameters

[14–17,37].

$$a = \sum_{i,j=1}^N \sqrt{a_i a_j} f_{ij}(T) (1 - k_{ij}) x_i x_j, \quad a_i = 0.427480 \frac{R^2 T_{ci}^2}{P_{ci}} \alpha_i(T). \quad (6)$$

$$f_{ij}(T) = 1 + \frac{\tau_{ij}}{T}, \quad \text{where } \tau_{ij} = \tau_{ji} \text{ and } \tau_{ii} = 0. \quad (7)$$

$$k_{ij} = \frac{l_{ij} l_{ji} (x_i + x_j)}{l_{ji} x_i + l_{ij} x_j}, \quad \text{where } k_{ii} = 0. \quad (8)$$

$$b = \frac{1}{2} \sum_{i,j=1}^N (b_i + b_j) (1 - k_{ij}) (1 - m_{ij}) x_i x_j, \quad b_i = 0.08664 \frac{RT_{ci}}{P_{ci}},$$

$$\text{where } m_{ij} = m_{ji} \text{ and } m_{ii} = 0. \quad (9)$$

$T_{ci}$ : critical temperature of the  $i$ th species;  $P_{ci}$ : critical pressure of the  $i$ th species;  $R$ : universal gas constant;  $x_i$ : mole fraction of the  $i$ th species.

In the above model, there are a maximum of four binary interaction parameters:  $l_{ij}$ ,  $l_{ji}$ ,  $m_{ij}$ , and  $\tau_{ij}$  for each binary pair. However, only two or three parameters are sufficient for most cases. The fugacity coefficient  $\phi_i$  of the  $i$ th species for the present EOS model, which is needed for the phase equilibrium calculation, is given by:

$$\ln \phi_i = \ln \frac{RT}{P(V-b)} + b'_i \left( \frac{1}{V-b} - \frac{a}{RTb(V+b)} \right) + \frac{a}{RTb} \left( \frac{a'_i}{a} - \frac{b'_i}{b} + 1 \right) \ln \frac{V}{V+b}, \quad (10)$$

where  $a'_i \equiv (\partial na / \partial n_i)_{n_{j \neq i}}$  and  $b'_i \equiv (\partial nb / \partial n_i)_{n_{j \neq i}}$ ;  $n$  = total mole number and  $n_i$  = mole number of  $i$ th species (or  $x_i = n_i/n$ ). The explicit forms of  $a'_i$  and  $b'_i$  may be useful for readers and are given as:

$$a'_i = 2 \sum_{j=1}^N \sqrt{a_i a_j} f_{ij} x_j \left\{ 1 - k_{ij} - \frac{l_{ij} l_{ji} (l_{ij} - l_{ji}) x_i x_j}{(l_{ji} x_i + l_{ij} x_j)^2} \right\} - a, \quad (11)$$

$$b'_i = \sum_{j=1}^N (b_i + b_j) (1 - m_{ij}) x_j \left\{ 1 - k_{ij} - \frac{l_{ij} l_{ji} (l_{ij} - l_{ji}) x_i x_j}{(l_{ji} x_i + l_{ij} x_j)^2} \right\} - b. \quad (12)$$

The equilibrium solubility for the ternary VLE system can be obtained by solving the following equilibrium conditions:

$$x_i \phi_i^L = y_i \phi_i^V \quad (i = 1, 2, 3), \quad (13)$$

where  $x_i$ : liquid mole fraction of the  $i$ th species ( $x_1 + x_2 + x_3 = 1$ );  $y_i$ : vapor mole fraction of the  $i$ th species ( $y_1 + y_2 + y_3 = 1$ );

$\phi_i^L$ : liquid-phase fugacity coefficient of the  $i$ th species;

$\phi_i^V$ : vapor-phase fugacity coefficient of the  $i$ th species.

In the case of three phase equilibria (VLE), equations corresponding to Eq. (13) become:

$$x_i^{L1} \phi_i^{L1} = x_i^{L2} \phi_i^{L2} = y_i^V \phi_i^V \quad (i = 1, 2, 3), \quad (14)$$

**Table 3**

EOS constants for pure compounds used in the present study.

	Hydrogen sulfide	Carbon dioxide	[bmim][PF <sub>6</sub> ] <sup>a</sup>
Molar mass/g mol <sup>-1</sup>	34.08	44.01	284.18
$T_c$ /K	373.60	304.13	860.5
$P_c$ /MPa	9.0080	7.377	2.645
$\beta_0$	0.99879	1.00049	1.0
$\beta_1$	0.33206	0.43866	0.62627
$\beta_2$	-0.049417	-0.10498	-
$\beta_3$	0.0046387	0.06250	-

<sup>a</sup> Taken from our previous work, see Ref. [37].

**Table 4**  
Optimal binary interaction parameters in Eqs. (7)–(9).

System (1)/(2)	$l_{12}$	$l_{21}$	$m_{12}=m_{21}$	$\tau_{12}=\tau_{21}/K$
CO <sub>2</sub> /[bmim][PF <sub>6</sub> ]	0.2725	0.2498	-0.2988	57.39
H <sub>2</sub> S/[bmim][PF <sub>6</sub> ]	0.2606	0.2170	-0.2400	69.16
CO <sub>2</sub> /H <sub>2</sub> S	0.04014	2.7134	0.0	-23.37

where superscripts, L1 and L2, denote one liquid phase (1) and another coexisting liquid phase (2) of VLE, respectively. Numerical solutions of Eq. (13) or Eq. (14) (non-linearly coupled equations) can be obtained by use of the TP-Flash (Rachford-Rice) method [38].

### 3.1. EOS model parameters

Pure component EOS parameters for hydrogen sulfide and carbon dioxide were determined based on data from Refs. [34,39], respectively. For the ionic liquid, the critical parameters ( $T_c$  and  $P_c$ ) and  $\beta_k$  in Eqs. (3)–(5) were taken from our previous work [37]. Table 3 shows the EOS constants for the present compounds. Binary interaction parameters,  $l_{ij}$ ,  $l_{ji}$ ,  $m_{ij}$ , and  $\tau_{ij}$  in Eqs. (7)–(9), for each binary pair were obtained using non-linear regression analyses of experimental  $PT_x$  (pressure–temperature composition) data for CO<sub>2</sub> + [bmim][PF<sub>6</sub>] [17], H<sub>2</sub>S + [bmim][PF<sub>6</sub>] [28] and CO<sub>2</sub> + H<sub>2</sub>S [13]

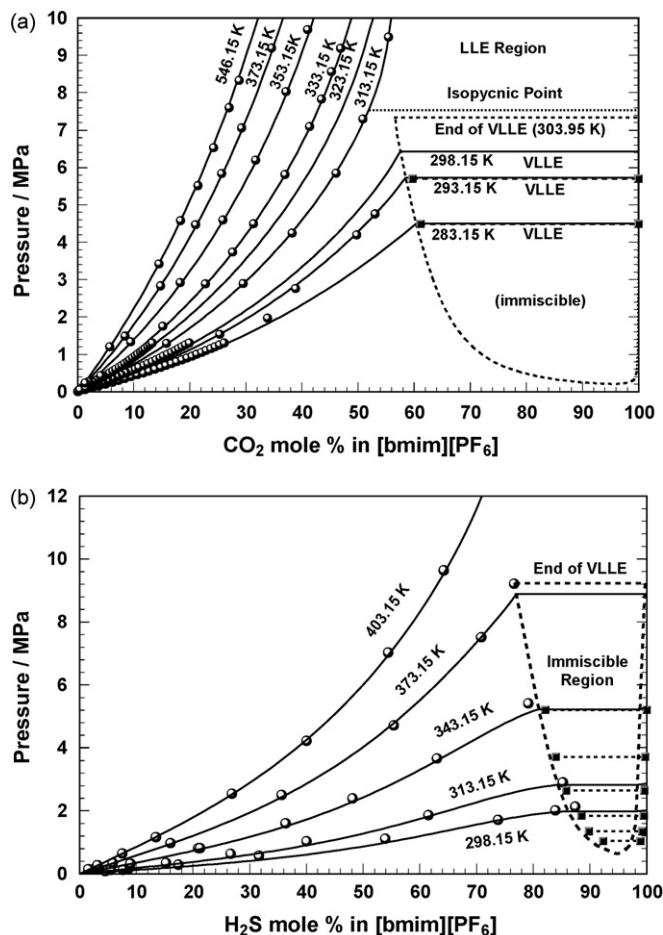


**Fig. 3.** Isothermal  $P_x$  (pressure–liquid composition) phase diagram. (a)  $P_x$  phase diagram of CO<sub>2</sub> + [bmim][PF<sub>6</sub>] binary system, taken from Ref. [17], symbols: filled squares present VLE data; (b)  $P_x$  phase diagram of H<sub>2</sub>S + [bmim][PF<sub>6</sub>] binary system, lines: the present EOS calculations, symbols: filled circles, experimental data taken from Ref. [28], filled squares, present VLE data.

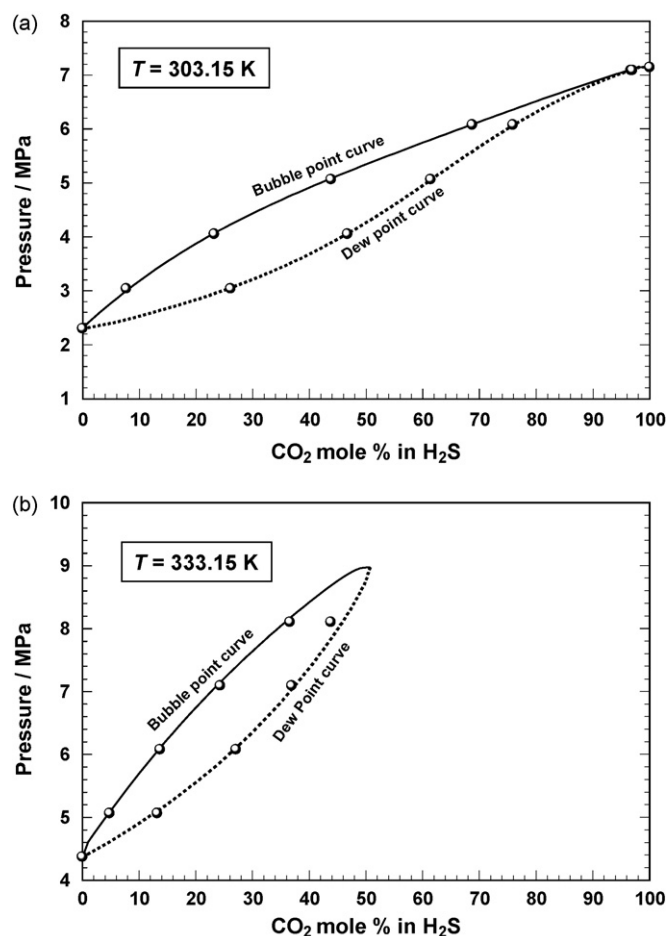


**Fig. 4.** Isothermal VLE  $P_{xy}$  (pressure–liquid–vapor composition) diagrams of the binary H<sub>2</sub>S/CO<sub>2</sub> system. Lines: the present EOS calculations; solid lines = bubble point curves; broken lines = dew point curves. Symbols: data from REFPROP program [34]. (a)  $T = 303.15$  K and (b)  $T = 333.15$  K.

systems. Table 4 presents optimal binary interaction parameters for the present system pairs.

### 3.2. EOS model validation

Fig. 3a is a  $PT_x$  phase diagram which shows our previous model predictions of CO<sub>2</sub> solubilities in [bmim][PF<sub>6</sub>] with the present VLE data. The standard deviation for the  $P$  versus  $x_1$  fit is excellent ( $dP = 0.017$  MPa). EOS model predictions have also been compared with the observed VLE data in Fig. 3a and are in excellent agreement with the experimental data shown at 283 and 293 K which suggest that this binary system is Type V phase behavior, according to the classification of von Konynenburg and Scott [40]. Our EOS model predicted the lower critical solution temperature (LCST) of about 197 K at 95.6 mol% of CO<sub>2</sub> in [bmim][PF<sub>6</sub>]. However, the VLE curve likely interferes with the solid–liquid equilibrium boundary because the CO<sub>2</sub>-rich liquid (top phase) in the samples containing 74.2 and 95.5 mol% CO<sub>2</sub> + [bmim][PF<sub>6</sub>] began to solidify when cooled to 198 K.

Fig. 3b shows a similar  $PT_x$  phase diagram of the H<sub>2</sub>S solubility measurements by Jou and Mather in [bmim][PF<sub>6</sub>] taken from Ref. [28]. The standard deviation for the  $P$  versus  $x_1$  fit is again excellent ( $dP = 0.036$  MPa). EOS model predictions have been compared with the observed VLE data shown at 273.6, 282.8, 294.6, 309.6, 325.2, and 342.2 K which suggest that this binary system also belongs to the Type V phase behavior. A cloud point was measured at  $254 \pm 5$  K with the sample containing 93.1 mol% of H<sub>2</sub>S in [bmim][PF<sub>6</sub>]. Based

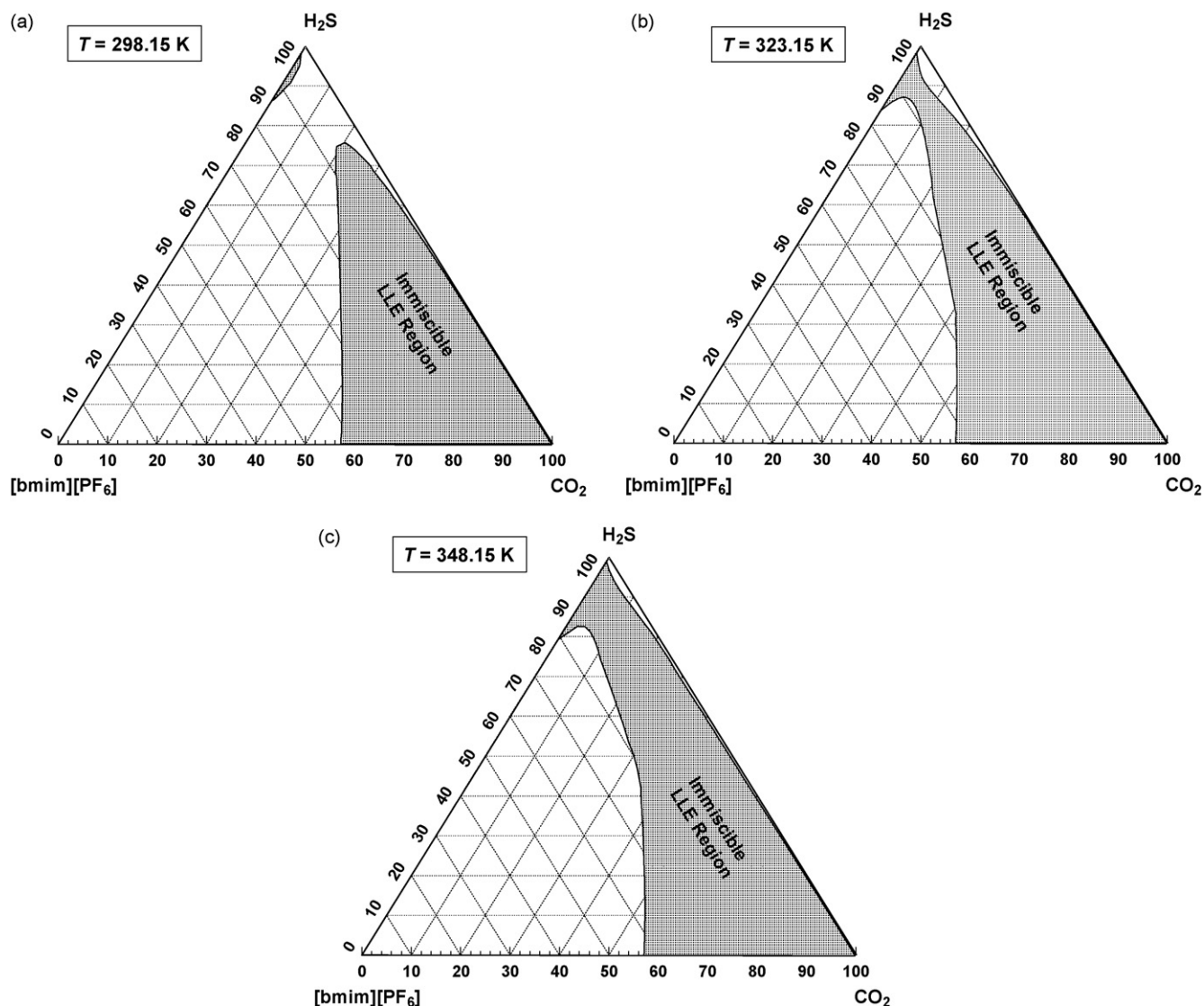


Fig. 5. Isothermal ternary CO<sub>2</sub>/H<sub>2</sub>S/[bmim][PF<sub>6</sub>] phase diagrams calculated by the present EOS model. (a) T = 298.15 K, (b) T = 323.15 K, and (c) T = 348.15 K.

**Table 5**  
Experimental VLE data for ternary mixtures.

Feed CO <sub>2</sub> /mol%	Feed H <sub>2</sub> S/mol%	Feed [bmim][PF <sub>6</sub> ]/mol%	T/K	P/MPa	Liquid H <sub>2</sub> S calculated/mol%	Liquid [bmim][PF <sub>6</sub> ] calculated/mol%	Vapor H <sub>2</sub> S calculated/mol%	Vapor H <sub>2</sub> S measured/mol%
69.3 ± 0.7	7.3 ± 0.1	23.4 ± 0.8	296.1	0.474	3.2 ± 0.1	88.9 ± 0.2	8.8 ± 0.2	9.2 ± 1.0 <sup>a</sup>
58.9 ± 0.8	6.2 ± 0.1	34.9 ± 0.9	296.1	0.460	2.9 ± 0.1	89.3 ± 0.2	8.3 ± 0.2	8.8 ± 1.0 <sup>a</sup>
48.5 ± 0.8	5.1 ± 0.1	46.4 ± 0.9	296.4	0.453	2.6 ± 0.1	89.7 ± 0.2	7.7 ± 0.3	8.3 ± 1.0 <sup>a</sup>
42.6 ± 0.5	35.5 ± 0.4	21.9 ± 0.8	296.2	0.543	18.7 ± 0.2	76.5 ± 0.3	42.2 ± 0.6	43.0 ± 1.0 <sup>b</sup>
27.9 ± 0.5	23.2 ± 0.4	48.9 ± 0.9	296.0	0.460	14.1 ± 0.1	81.2 ± 0.2	37.0 ± 1.0	38.8 ± 1.0 <sup>b</sup>
19.1 ± 0.4	15.9 ± 0.3	65.1 ± 0.7	296.3	0.425	11.2 ± 0.1	84.0 ± 0.2	32.1 ± 1.0	33.4 ± 1.0 <sup>b</sup>
7.6 ± 0.1	71.9 ± 0.7	20.5 ± 0.8	296.1	0.494	33.9 ± 0.6	65.1 ± 0.7	89.4 ± 0.3	89.5 ± 1.0 <sup>c</sup>
8.4 ± 0.1	79.9 ± 0.7	11.7 ± 0.7	296.0	0.494	34.2 ± 0.4	64.9 ± 0.4	90.0 ± 0.2	90.0 ± 1.0 <sup>c</sup>
5.1 ± 0.1	48.7 ± 0.8	46.2 ± 0.9	296.0	0.446	30.7 ± 0.4	68.3 ± 0.5	86.4 ± 0.7	87.7 ± 1.0 <sup>c</sup>
4.3 ± 0.1	40.7 ± 0.7	55.0 ± 0.8	294.8	0.343	25.3 ± 0.6	73.8 ± 0.5	85.7 ± 0.8	86.9 ± 1.0 <sup>c</sup>
48.5 ± 0.8	5.1 ± 0.1	46.4 ± 0.9	322.7	0.501	1.7 ± 0.2	93.2 ± 0.1	8.5 ± 0.3	8.9 ± 1.0 <sup>a</sup>
27.9 ± 0.5	23.2 ± 0.4	48.9 ± 0.9	322.7	0.536	9.2 ± 0.1	87.5 ± 0.1	40.9 ± 0.9	41.2 ± 1.0 <sup>b</sup>
19.1 ± 0.4	15.9 ± 0.3	65.1 ± 0.7	322.5	0.515	8.1 ± 0.1	88.5 ± 0.1	37.5 ± 1.0	37.6 ± 1.0 <sup>b</sup>
5.1 ± 0.1	48.7 ± 0.8	46.2 ± 0.9	322.4	0.550	20.9 ± 0.3	78.5 ± 0.4	88.6 ± 0.5	88.7 ± 1.0 <sup>c</sup>
4.3 ± 0.1	40.7 ± 0.7	55.0 ± 0.8	322.3	0.419	16.2 ± 0.3	83.3 ± 0.3	88.4 ± 0.6	89.3 ± 1.0 <sup>c</sup>

Liquid CO<sub>2</sub> mol% = (100 – liquid H<sub>2</sub>S mol% – liquid [bmim][PF<sub>6</sub>] mol%). Vapor CO<sub>2</sub> mol% = (100 – vapor H<sub>2</sub>S mol%), and vapor [bmim][PF<sub>6</sub>] = 0 mol%.

<sup>a</sup> CO<sub>2</sub>/H<sub>2</sub>S gas mixtures: 90.4/9.6 mol%.

<sup>b</sup> CO<sub>2</sub>/H<sub>2</sub>S gas mixtures: 54.6/45.4 mol%.

<sup>c</sup> CO<sub>2</sub>/H<sub>2</sub>S gas mixtures: 9.5/90.5 mol%.

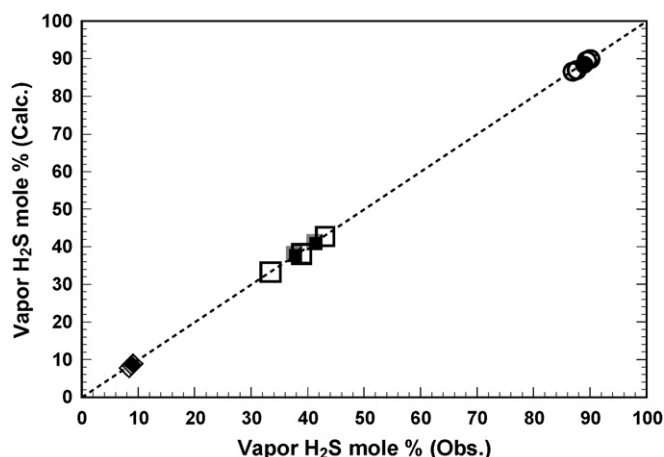


**Fig. 6.** Comparison of experimental and calculated VLE data for the ternary  $\text{CO}_2/\text{H}_2\text{S}/[\text{bmim}][\text{PF}_6]$  system. Calculated vapor-phase compositions of  $\text{H}_2\text{S}$  ( $\text{CO}_2$  mol% =  $100 - \text{H}_2\text{S}$  mol%) are compared with observed  $\text{H}_2\text{S}$  vapor compositions for various experimental conditions (see Table 5). Symbols: open symbols = about 296 K; solid symbols = about 322 K; circle symbols = 9.5/90.5 mol%  $\text{CO}_2/\text{H}_2\text{S}$  feed; square symbols = 54.6/45.4 mol%  $\text{CO}_2/\text{H}_2\text{S}$  feed; diamond symbols = 90.4/9.6 mol%  $\text{CO}_2/\text{H}_2\text{S}$  feed.

on the EOS model and the VLE measurements we calculate a LCST of about 258 K at 95 mol% of  $\text{H}_2\text{S}$  in  $[\text{bmim}][\text{PF}_6]$ . However, the lack of a cloud point for the sample containing 95.5 mol% of  $\text{H}_2\text{S}$  in  $[\text{bmim}][\text{PF}_6]$  may suggest two phases exist in a narrow region at low temperature. Possible explanations for the persistence of the two phases at low temperature include: the  $[\text{bmim}][\text{PF}_6]$  becomes highly viscous and the sample may not have been properly mixed, the system may be metastable, or critical slowdown is occurring.

Vapor liquid equilibrium (VLE) data of  $\text{CO}_2 + \text{H}_2\text{S}$  mixtures obtained from Ref. [13] are shown in Fig. 4a and b for selected isotherms (303.15 and 333.15 K), compared with the present EOS calculations. It should be noted that no VLE exists at 333.15 K above about 50 mol%  $\text{CO}_2$  in  $\text{H}_2\text{S}$ . Although the solubility behavior of each binary system has been well correlated with the present EOS model as illustrated in Figs. 3 and 4, the phase behavior prediction of the ternary system of  $\text{CO}_2/\text{H}_2\text{S}/[\text{bmim}][\text{PF}_6]$  may not always be guaranteed based on the binary interaction parameters alone. Particularly for systems containing supercritical fluids and/or non-volatile compounds such as the present case, the validity of a proposed EOS model for ternary mixtures must be checked experimentally. Isothermal ternary phase diagrams predicted by the present EOS at 298.15, 323.15 and 348.15 K are shown in Fig. 5, where a large portion of the ternary composition exhibits the liquid-liquid separation (LLE) that reflects the immiscibility gap in the binary  $\text{CO}_2 + [\text{bmim}][\text{PF}_6]$  and  $\text{H}_2\text{S} + [\text{bmim}][\text{PF}_6]$  systems; see Fig. 3a and b.

Fig. 6 presents the comparison of observed and calculated values for  $\text{H}_2\text{S}$  mole % in the vapor phase ( $\text{CO}_2$  mol% =  $100 - \text{H}_2\text{S}$  mol%, and  $[\text{bmim}][\text{PF}_6] = 0$  mol%) under various  $T, P$ , and feed composition conditions; see Table 5. The model calculations and experimental data are in excellent agreement ( $<1.0$  mol%).

#### 4. Results and discussion

Now that the present EOS model has been verified, we can predict the solubility behavior of the present ternary system with confidence. In order to assess the feasibility of the gas separation by the extractive distillation or selective absorption method, gaseous selectivity  $\alpha_{A/B}$ , ability to separate gases A and B in the gas phase, or gaseous absorption selectivity  $S_{B/A}$  in the liquid phase is commonly

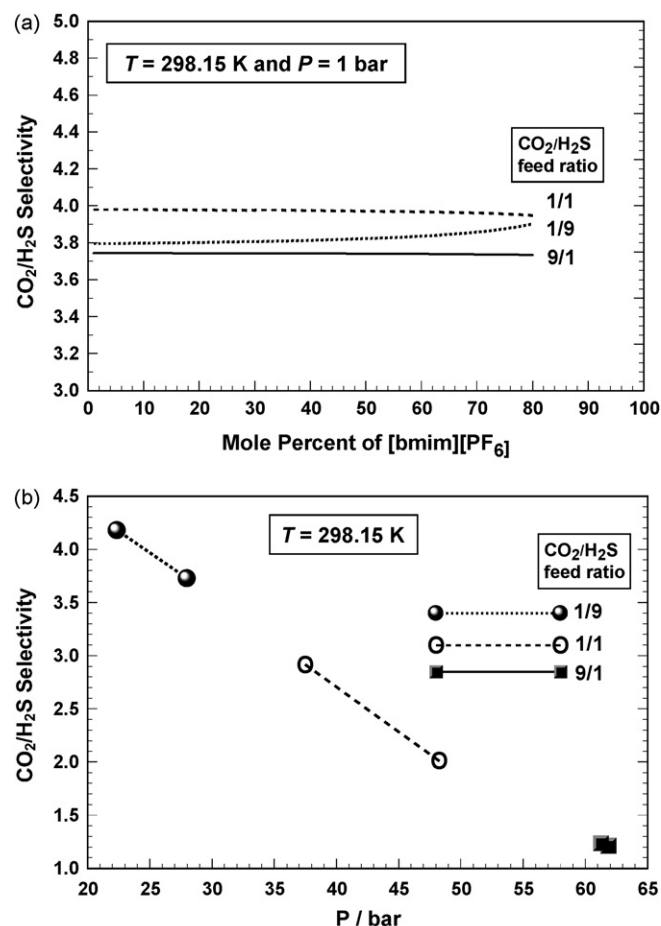


**Fig. 7.** (a) Plots of calculated selectivity defined by Eq. (15) versus  $[\text{bmim}][\text{PF}_6]$  mole percent with three different  $\text{CO}_2/\text{H}_2\text{S}$  feed ratios at  $T = 298.15$  K and  $P = 1$  bar. (b) Selectivity plots without ionic liquid  $[\text{bmim}][\text{PF}_6]$  as a function of total pressure. Three cases with different  $\text{CO}_2/\text{H}_2\text{S}$  feed ratios are shown at  $T = 298.15$  K. Lines: dotted line = 1/9  $\text{CO}_2/\text{H}_2\text{S}$  feed mole ratio; broken line = 1/1  $\text{CO}_2/\text{H}_2\text{S}$  feed mole ratio; solid line = 9/1  $\text{CO}_2/\text{H}_2\text{S}$  feed mole ratio.

defined as in Refs. [41–43]:

$$\alpha_{A/B} = S_{B/A} = \frac{y_A/x_A}{y_B/x_B} \quad (15)$$

where  $x_A$  (or  $x_B$ ) and  $y_A$  (or  $y_B$ ) are the mole fractions of A (or B) in the ionic liquid solution phase and vapor phase, respectively. Here we denote  $\text{CO}_2$  as A and  $\text{H}_2\text{S}$  as B. The  $\text{CO}_2/\text{H}_2\text{S}$  selectivity ( $\alpha_{A/B}$ ) in the gas phase has been examined using the present EOS model at various  $T, P$ , and feed compositions, and results are shown in Figs. 7 and 8.

In Fig. 7a, the  $\text{CO}_2/\text{H}_2\text{S}$  selectivity ( $\alpha_{A/B}$ ) is plotted as a function of the ionic liquid  $[\text{bmim}][\text{PF}_6]$  concentration for ternary mixtures with three  $\text{CO}_2/\text{H}_2\text{S}$  mole ratios (1/9, 1/1 and 9/1) at  $T = 298.15$  K and  $P = 1$  bar. For all three cases, the selectivity ( $\alpha_{A/B}$ ) remains relatively constant at about 3.7–4.0 with increasing ionic liquid concentration. In order to understand the change in selectivity due to the ionic liquid addition, Fig. 7b provides clear insights, where the selectivity without  $[\text{bmim}][\text{PF}_6]$  at 298.15 K is plotted as a function of pressure for the same  $\text{CO}_2/\text{H}_2\text{S}$  feed ratios (1/9, 1/1, and 9/1). The selectivity enhancement due to the ionic liquid addition can be well observed from the comparison between Fig. 7a and b. For example, the feed ratio of 9/1 ( $\text{CO}_2/\text{H}_2\text{S}$ ) with the ionic liquid has a selectivity of about 3.7, while the corresponding case without the ionic liquid shows a selectivity of about 1.2. As the feed ratio decreases (9/1 to 1/1 to 1/9  $\text{CO}_2/\text{H}_2\text{S}$ ) the improvement in selectivity with the ionic liquid versus without the ionic liquid also decreases.

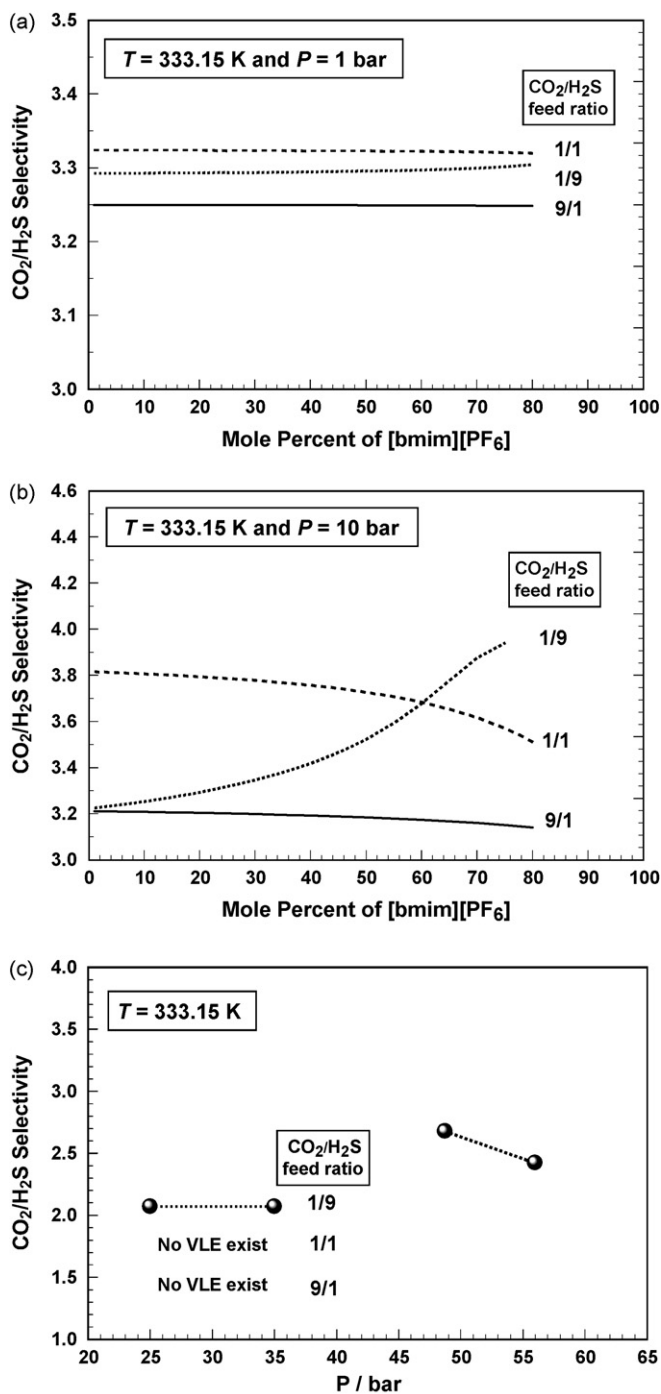


**Fig. 8.** Plots of calculated selectivity defined by Eq. (15) versus [bmim][PF<sub>6</sub>] mole percent with three different CO<sub>2</sub>/H<sub>2</sub>S feed ratios at (a)  $T = 333.15$  K and  $P = 1$  bar, (b)  $T = 333.15$  K and  $P = 10$  bar. (c) Selectivity plots without ionic liquid [bmim][PF<sub>6</sub>] as a function of total pressure. Three cases with different CO<sub>2</sub>/H<sub>2</sub>S feed ratios are shown at  $T = 333.15$  K. Lines: dotted line = 1/9 CO<sub>2</sub>/H<sub>2</sub>S feed mole ratio; broken line = 1/1 CO<sub>2</sub>/H<sub>2</sub>S feed mole ratio; solid line = 9/1 CO<sub>2</sub>/H<sub>2</sub>S feed mole ratio.

The selectivity characteristics at a higher temperature (333.15 K) and pressures (1 and 10 bar) are shown in Fig. 8, with and without the ionic liquid addition. The general behavior as shown in Fig. 8 is similar to the case in Fig. 7; however the selectivity enhancement with the ionic liquid addition is lower. The most important fact to consider at higher temperature is at high CO<sub>2</sub>/H<sub>2</sub>S feed ratios (1/1 and 9/1) without the ionic liquid no VLE exists and the gas mixtures cannot be separated using traditional distillation methods as shown in Fig. 8c. Therefore, only

with the addition of the ionic liquid as shown in Fig. 8a and b is separation of CO<sub>2</sub> and H<sub>2</sub>S possible.

Finally, it should be mentioned that negative excess molar volumes in [bmim][PF<sub>6</sub>]-rich side solutions have been observed for both the CO<sub>2</sub> and H<sub>2</sub>S binary systems. In the case of the CO<sub>2</sub> + [bmim][PF<sub>6</sub>] and H<sub>2</sub>S + [bmim][PF<sub>6</sub>] binary systems the ionic liquid rich side solution molar volumes are largely negative (e.g.  $-6$  to  $-9$  cm<sup>3</sup> mol<sup>-1</sup>) and (e.g.  $-2$  to  $-11$  cm<sup>3</sup> mol<sup>-1</sup>), respectively. These values are similar to our previous studies of other binary systems containing CO<sub>2</sub> + ionic liquids (e.g. [hmim][Tf<sub>2</sub>N] and [bmim][acetate]) [14,15] and hydrofluorocarbons (HFCs) + ionic liquids [35,36,39]. This clearly indicates that RTILs with gases such as CO<sub>2</sub>, H<sub>2</sub>S and HFCs have quite large negative excess molar volumes compared with what have been reported with ordinary liquid mixtures (typically about  $0$  to  $\pm 3$  cm<sup>3</sup> mol<sup>-1</sup>) [44]. This poses a unique and interesting challenge for theoretical modelers to explain this phenomenon. One possible explanation by Huang et al. [45] for the CO<sub>2</sub> + [bmim][PF<sub>6</sub>] system indicates that small angular rearrangements of the anion are occurring which create localized cavities that allow CO<sub>2</sub> to fit above and below the imidazolium ring without much change from the molar volume of pure [bmim][PF<sub>6</sub>]. Similar rearrangements maybe occurring with H<sub>2</sub>S and HFCs in RTILs as well as an additional force such as hydrogen bonding may also be involved.

## 5. Conclusions

Although the separation concept of gaseous mixtures using room-temperature ionic liquids has been proposed in the past, no quantitative demonstrations have been reported in the literature for CO<sub>2</sub>/H<sub>2</sub>S. In this report, we have developed for the first time a reliable EOS model for the ternary CO<sub>2</sub>/H<sub>2</sub>S/[bmim][PF<sub>6</sub>] system, and have examined the gaseous selectivity of these acid gases, using ionic liquid [bmim][PF<sub>6</sub>].

The present ionic liquid is not necessarily the best choice for the gaseous separation and/or capturing of CO<sub>2</sub> and H<sub>2</sub>S. The method presented here with a particular ionic liquid is merely a demonstration for such applications. However, it is shown that the present ionic liquid can affect the gaseous selectivity and future work will explore more optimal ionic liquid choices.

### List of symbols

$a$ and $b$	adjustable parameters, generic Redlich-Kwong EOS, Eq. (2)
$l_{ij}$ , $l_{ji}$ , and $m_{ij}$	binary interaction parameters, Eqs. (8)–(9)
$n$	total mole number
$n_i$	mole number of $i$ th species (or $x_i = n_i/n$ )
$P$	pressure (MPa)
$R$	gas constant ( $8.314472$ J mol <sup>-1</sup> K <sup>-1</sup> )
$T$	absolute temperature (K)
$V_i$	molar volume of $i$ th species (cm <sup>3</sup> mol <sup>-1</sup> , or m <sup>3</sup> mol <sup>-1</sup> )
$x_i$ and $y_i$	mole fractions of $i$ th species

### Greek characters

$\beta_k$	generic Redlich-Kwong EOS constants, Eq. (5)
$\phi_i$	fugacity coefficient of $i$ th species Eq. (10)
$\delta x$	uncertainty mole fraction and molar volume
$\alpha_{A/B}$	gas phase selectivity, Eq. (15)
$\tau_{ij}$	binary interaction parameter, Eq. (7) (K)

### Subscripts

A	CO <sub>2</sub>
B	H <sub>2</sub> S
$i$	$i$ th species
$m$	mixture

1	sample gas
2	ionic liquid
c	critical
r	reduced
TE	total error
RE	random error
SE	systematic error

#### Superscripts

–	molar property
E	excess property
'	lower phase, Eq. (1)
0	pure component, Eq. (1)
L1	liquid 1, Eq. (14)
L2	liquid 2, Eq. (14)
v	vapor, Eqs. (13)–(14)

#### Acknowledgements

The authors thank Mr. Brian L. Wells for his assistance in the vapor–liquid equilibrium measurements, Mrs. Anne Marie S. Niehaus for her assistance with the vapor–liquid–liquid equilibrium measurements, Mr. Gary W. Foggin for the schematic diagram of the sample cell, and DuPont Central Research and Development for supporting the present work.

#### References

- [1] D. Speyer, V. Ermatchkov, G. Maurer, *J. Chem. Eng. Data* 55 (2010) 283–290.
- [2] A. Böttger, V. Ermatchkov, G. Maurer, *J. Chem. Eng. Data* 54 (2009) 1905–1909.
- [3] B.P. Mandal, A.K. Biswas, S.S. Bandyopadhyay, *Sep. Purif. Technol.* 35 (2004) 191–202.
- [4] B.P. Mandal, S.S. Bandyopadhyay, *Chem. Eng. Sci.* 60 (2005) 6438–6451.
- [5] J.I. Lee, F.D. Otto, A.E. Mather, *J. Chem. Eng. Data* 20 (1975) 161–163.
- [6] I.-S. Jane, M.-H. Li, *J. Chem. Eng. Data* 42 (1997) 98–105.
- [7] R.D. Deshmukh, A.E. Mather, *Chem. Eng. Sci.* 36 (1981) 355–362.
- [8] G. Kuranov, B. Rumpf, N.A. Smirnova, G. Maurer, *Ind. Eng. Chem. Res.* 35 (1996) 1959–1966.
- [9] Á. Pérez-Salado Kamps, A. Balaban, M. Jödecke, G. Kuranov, N.A. Smirnova, G. Maurer, *Ind. Eng. Chem. Res.* 40 (2001) 696–706.
- [10] A. Finotello, J.E. Bara, D. Camper, R.D. Noble, *Ind. Eng. Chem. Res.* 47 (2008) 3453–3459.
- [11] B.J. Mayland, Removal of carbon dioxide and hydrogen sulfide from gaseous mixtures. U.S. Patent 3,275,403, 1966.
- [12] H.E. Benson, Separation of carbon dioxide and hydrogen sulfide from gas mixtures. U.S. Patent 3,642,430, 1972.
- [13] J.A. Bierlein, W.B. Kay, *Ind. Eng. Chem.* 45 (1952) 618–624.
- [14] M.B. Shiflett, A. Yokozeki, *J. Phys. Chem. B* 111 (2007) 2070–2074.
- [15] M.B. Shiflett, D.J. Kasprzak, C.P. Junk, A. Yokozeki, *J. Chem. Thermodyn.* 40 (2008) 25–31.
- [16] A. Yokozeki, M.B. Shiflett, C.P. Junk, L.M. Grieco, T. Foo, *J. Phys. Chem. B* 112 (2008) 16654–16663.
- [17] M.B. Shiflett, A. Yokozeki, *Ind. Eng. Chem. Res.* 44 (2005) 4453–4464.
- [18] Á. Pérez-Salado Kamps, D. Tuma, J. Xia, G. Maurer, *J. Chem. Eng. Data* 48 (2003) 746–749.
- [19] P. Husson-Borg, V. Majer, M.F. Costa Gomes, *J. Chem. Eng. Data* 48 (2003) 480–485.
- [20] A. Shariati, C.J. Peters, *J. Supercrit. Fluids* 30 (2004) 139–144.
- [21] A. Shariati, K. Gutkowski, C.J. Peters, *AIChE J.* 51 (2005) 1532–1540.
- [22] P. Scovazzo, D. Camper, J. Hieft, J. Poshusta, C. Koval, R. Noble, *Ind. Eng. Chem. Res.* 43 (2004) 6855–6860.
- [23] Z. Liu, W. Wu, B. Han, Z. Dong, G. Zhao, J. Wang, T. Jiang, G. Yang, *Chem. Eur. J.* 9 (2003) 3897–3903.
- [24] S.N.V.K. Aki, B.R. Mellein, E.M. Saurer, J.F. Brennecke, *J. Phys. Chem. B* 108 (2004) 20355–20365.
- [25] L.A. Blanchard, G. Gu, J.F. Brennecke, *J. Phys. Chem. B* 105 (2001) 2437–2444.
- [26] M.B. Shiflett, A. Yokozeki, *J. Chem. Eng. Data* 54 (2009) 108–114.
- [27] P.J. Carvalho, V.H. Álvarez, B. Schröder, A.M. Gil, I.M. Marrucho, M. Aznar, L.M.N.B.F. Santos, J.A.P. Coutinho, *J. Phys. Chem. B* 113 (2009) 6803–6812.
- [28] F.-Y. Jou, A.E. Mather, *Int. J. Thermophys.* 28 (2007) 490–495.
- [29] C.S. Pomelli, C. Chiappe, A. Vidis, G. Laurenczy, P.J. Dyson, *J. Phys. Chem. B* 111 (2007) 13014–13019.
- [30] Y.J. Heintz, L. Sehabiague, B.I. Morsi, K.L. Jones, D.R. Luebke, H.W. Pennline, *Energy Fuels* 23 (2009) 4822–4830.
- [31] A.H. Jalili, M. Rahmati-Rostami, C. Ghotbi, M. Hosseini-Jenab, A.N. Ahmadi, *J. Chem. Eng. Data* 54 (2009) 1844–1849.
- [32] A. Yokozeki, *Int. J. Thermophys.* 22 (2001) 1057–1071.
- [33] M.B. Shiflett, A. Yokozeki, *AIChE J.* 52 (2006) 1205–1219.
- [34] E.W. Lemmon, M.O. McLinden, M.L. Huber, Standard Reference Data Program REFPROP, version 8.0, National Institute of Standards and Technology, Gaithersburg, MD, 2008.
- [35] M.B. Shiflett, A. Yokozeki, *J. Phys. Chem. B* 110 (2006) 14436–14443.
- [36] M.B. Shiflett, A. Yokozeki, *J. Chem. Eng. Data* 51 (2006) 1931–1939.
- [37] A. Yokozeki, M.B. Shiflett, *AIChE J.* 52 (2006) 3952–3957.
- [38] H.C. Van Ness, M.M. Abbott, *Classical Thermodynamics of Nonelectrolyte Solutions*, McGraw-Hill, New York, 1982, p. 427.
- [39] R. Span, W. Wagner, *J. Phys. Chem. Ref. Data* 25 (1996) 1509–1596.
- [40] P.H. van Konynenburg, R.L. Scott, *Philos. Trans. A* 298 (1980) 495–540.
- [41] A. Yokozeki, M.B. Shiflett, *Appl. Energy* 84 (2007) 351–361.
- [42] A. Yokozeki, M.B. Shiflett, *Ind. Eng. Chem. Res.* 47 (2008) 8389–8395.
- [43] X. Peng, W. Wang, R. Xue, Z. Shen, *AIChE J.* 52 (2006) 994–1003.
- [44] J.S. Rowlinson, F.L. Swinton, *Liquids and Liquid Mixtures*, 3rd ed., Butterworth, London, 1982.
- [45] X. Huang, C. Margulis, Y. Li, B.J. Berne, *J. Am. Chem. Soc.* 127 (2005) 17842–17851.